Modelling, Measurement and Control C
Vol. 79, No. 3, September, 2018, pp. 83-89
Journal homepage: http://iieta.org/Journals/MMC/MMC_C

# Modelling and simulating a thermal storage system for the Savona campus smart polygeneration micro grid

Massimo Brignone[1], Federico Delfino[1], Francesco Devia[2], Marco Fossa[2*], Fabio Pampararo[1]

[1] DITEN Dept. Dept. University of Genova, via Opera Pia 11a, Genova 16145, Italy
[2] DIME Dept. University of Genova, via Opera Pia 15a, Genova 16145, Italy

Corresponding Author Email: marco.fossa@unige.it

https://doi.org/10.18280/mmc_c.790304

**Received:** 28 April 2018
**Accepted:** 29 May 2018

***Keywords:***
*thermal energy storage, smart grid, polygeneration, optimization and control*

**ABSTRACT**

The present paper is addressed to a further development of the Energy Management System (EMS) which is implemented and running at the Smart Polygeneration Microgrid (SPM) at the Savona Campus of the University of Genova. The SPM thermal network is constituted by heat generation units (cogenerative gas turbines and gas boilers, overall thermal power about 1MWth) and a network of pipelines providing the heat to a series of buildings during the daily working hours. Being the electric power demand significantly present also at night, a heat storage system would be advisable for full cogeneration all day long. For this reason the existing EMS model and predictive control has been modified for taking into account the presence of a thermal storage system of suitable volume. The new operation scheme at simulation level also includes a biomass burner, to be switched on in priority with respect to the existing gas burners. The approach for modelling the heat storage, in terms mainly of storage energy content, allows the economic feasibility of the investment to be assessed when subhourly simulations of real operating conditions are performed with respect to recent historical time series of electric and heat load demand at the Savona Campus.

## 1. INTRODUCTION

Energy storages are one of the key components that makes it possible to exploit low impact energy sources to fulfill customer needs, in terms of time, location, amount and kind of energy. They play a vital role in integration of different energy grids and favor a good neighborhood policy among energy suppliers. Additional benefits are related to users who can reduce their energy bills and the impact at environmental level. Finally the flexibility of the overall grid is enhanced and the initial and maintenance costs can be lowered [1]. Among the different type of Thermal energy Storages (TS), daily storages are of particularly interesting because of their low capital investments, reduced size, ease of manufacturing and, last but not least, the sizing of daily storage for applications is not as critical as sizing larger annual storages.

Among the most promising type energy storages that are currently available, TS continue to play an interesting role because of their low cost, simplicity and ease of maintenance. Commonly, TSs are used as interface between the final thermal users and the complex energy grid and they are intended to make possible an active demand management (ADM) of energy consumption. Indeed, the effectiveness of TS has a direct impact on user consumption. The search for integration and different energy sources and energy has risen, higher and higher, the interest in TS for exploiting renewables [2]. First of all, the goal of a TS is decoupling the time profile of energy suppliers from the consumer one. Nevertheless, in most of applications, TS has second purpose that has not a minor importance. Also in simpler system, like for instance Water TSs and Sensible Heat TSs are, there is a set of small arrangements aimed at optimizing the temperature of the streams flowing both towards the supplier subnetworks and to the consumer ones. It is worth noting that these devices are intended to increase the effectiveness of the whole plant and that they must be evaluated from this point of view [3].

Effective performance of TS are strongly linked to the possibility of maintaining the thermal stratification. Stratification is generally devoted to make independent the temperatures of the streams flowing in and out of the TS and hence to maintain the original exergy levels inside the storage. In these cases, the TS works better than simple reservoir and their performance are higher than the ones that can be calculated by simple models, at lumped parameters.

The presence of an effective thermal stratification of the fluid inside of a tank, depends on the stability of the temperature distribution along the vertical axis: a warmer volume, in the upper part of the tank, a cooler zone beneath it, and a thermocline region, between them, where temperature vertical gradients are higher. This structure is stable as far as conduction in fluid and the mixing and turbulence do not prevail: all the above conditions move the TS to temperature uniformity.

The effect of turbulence is relevant and a wide literature is available about it, such as [4], which addresses the definition of the parameters of turbulence models, in order to obtain an accurate description of the vertical temperature distribution in TS.

Moreover, there is a large number of parameters that affect thermal stratification, such as the shape of the tank [5], the mass flow rate [6], the location and the shape of the inlet and outlet ports and also the presence of baffles inside the tank aimed at preventing mixing [7]. It is a well-established practice to insert some properly shaped partitions inside of the storage to improve stratification. Some authors [8] tested the effectiveness of four different baffles on stratification in a small TS, using various performance indexes.

A large number of detailed CFD analysis of TSs is available in literature, but the need of simple, fast and accurate models led some authors [9] to develop and refine simpler models, adjusting a Matlab model with the results of a detailed CFD analysis. In particular, this model is specially fit to account for the mixing induced by the incoming flows.

When the computational efficiency is mandatory, such as during an optimized design process or for control issues, it is a good approach to use simpler mathematical models that can account for stratification, without losing the major physical aspects of the thermal phenomena. These simple models despite their intrinsic, lower order of precision and accuracy allow fast predictions on the TS behavior in time. Among these simple models, the battery models take into account the flows of energy into the TS and separate the hot to the cold streams, as in a perfect stratification at two temperature levels. Some papers show that even a low order battery model gives more accurate results than the fully mixed one: the error on the feeding temperature out of the TS is lower than 10% for a battery model while can be up to 50% the fully mixed one[10].

Rosen in [11] compares the results obtained dividing TS into 2, 20 and 200 volumes, considering constant, linear and stepped distribution of temperature in each volume. The authors calculate the effect of the model assumptions on the value of the performance indexes calculated with each model. This work shows that the battery model is sufficiently accurate in calculating most of the performance indexes, with an error lower than 5%, apart from the calculation of the difference between the real TS energy and the one of a corresponding perfectly mixed one, which can be up to 33%.

In this frame, the work of Haller et al, [3], is very interesting because it presents an extended review of the methods for assessing the stratification efficiency in TS.

A large number of indexes has been and used [12] to describe the quality of the thermal stratification in tanks, but it is very difficult to quantify their effective advantages in analyzing the performance of TSs

Njoku et al. [13] make an interesting analysis of the performance of stratified sensible thermal energy stores on the basis of various thermodynamic functions and also report an interesting list of references, which recommends the definition of various and complex indexes to quantify the of the increase in performance related to stratification, in a TS.

On the basis of current literature, it is possible to state that a battery model (double temperature model) is the one that better fits specific requirements of control and regulation systems devoted to complex thermal plants.

In the present paper the Energy Management System (EMS) of the Smart Polygeneration grid of the University of Genova, Italy, is described and a new algorithm for assessing the effects of a new TS to be inserted into the plant are discussed. The analysis allowed the best size of the storage to be estimated based on a series of simulations related to historical series of subhourly heat demand profiles

## 2. THE SMART POLYGENERATION MICROGRID AT THE UNIVERSITY OF GENOVA

In this section, all the electrical and thermal components of the SPM will be described (see [14] for details).

As concern the electric part, the SPM is fed by a secondary substation 15kV/400V, which provides together with the power generated inside the microgrid to satisfy the electrical load of the Savona Campus. As shown in Fig. 1, the main technologies of the SPM can be resumed as follows:

(1) two different kind of renewable energy sources:

(2) three Concentrating Solar Power (CSP) units able to produce 1 kW of electrical power and 3 kW of thermal power (each);

(3) two photovoltaic (PV) fields (80 kW of peak);

(4) two Cogenerative Gas Turbine (CGT) units (Capstone C65), each one able to produce 65 kW of electrical power and 130 kW of thermal power;

(5) an electrical storage (ES) unit based on SoNick batteries by FIAMM S.p.A with size of 141 kWh;

(6) two recharging stations for electric vehicles;

(7) an absorption chiller ($H_2O$/LiBr technology) having a cooling rated power of 70 kW;

(8) two Gas Heaters (GH) able to produce 1000 kW of thermal power and used as a backup.

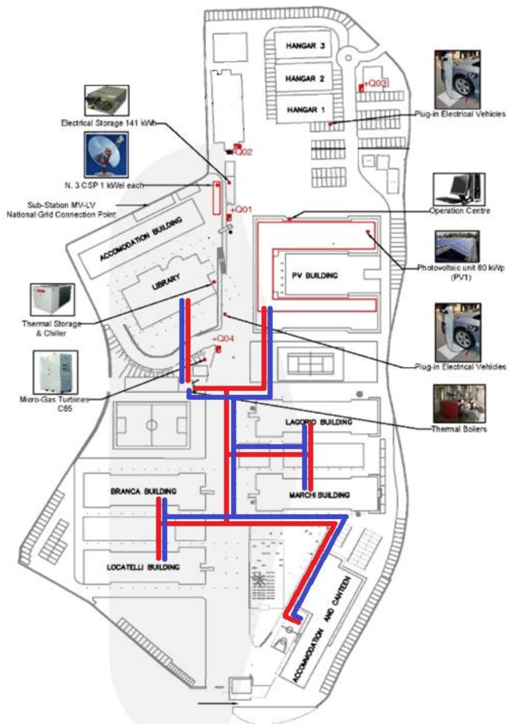


**Figure 1.** The layout of the SPM at the Savona Campus of the University of Genova, Italy. Photovoltaic strings (PV), Cogenerative Gas Turbines (CGT), back up Gas Heater (GH), Electric Storage (ES). The red and blue lines represent the thermal network that fed the Campus

All the described components are controlled and monitored by a SCADA system based on WINCC software and an Energy Management System (EMS) allows to optimally manage the microgrid. The communication between the microgrid and the supervisor system has been done by means of a double fiber optic ring which connects the server with the switches located in each switchboard, where TM 1703 ACP

Remote Terminal Units (RTU) and I/O modules are installed. In Fig. 1 also the thermal network of the SPM is sketched by red and blue lines, respectively corresponding to the supply lines, driving the hot water from the heating station to each building of the Campus, and to the return lines, driving back the cold water from the users to the heating plants. The thermal network is fed by the cogeneration gas turbines and the two gas heater. The pipes, properly insulated in order to minimize losses; have been underground installed and their diameters are in the range between DN80 and DN125. Inside each building, hot water is moved by on/off centrifugal pumps and heat is transferred to the indoor air by means of radiators or fan coils.

The heating network is real-time monitored from supervisor system by means of on-field sensors able to measure the water mass flow rate, the supply and return lines temperatures, the thermal power output of each gas turbine and gas heater, and the outdoor temperature. In this way it is possible to monitoring the whole thermal load of the Campus, which, in coldest winter days, can reach 900 kW of peak.

## 3. SPM COMPONENT MODELLING AND OPERATIONAL COST DEFINITION

In this section the models of the units that contribute to the production of thermal energy in the SPM will be described. Together with the currently installed components, also the biomass boiler and the thermal storage models will be presented, in order to evaluate their affordability in the SPM.

From here on, *t* denotes the generic timeframe and *Δt* is the length of each time interval, that for sake of simplicity it will be supposed to be constant during the whole period.

### 3.1 Renewable Energy Sources (RES)

PV unit and CSP, are basically known active power injections $P^{el}_{RES,t}$, function of the solar irradiance and the temperature.

### 3.2 Cogenerative Gas Turbine (CGT)

The CGT unit can be described at the time sample *t* with three main variables: the primary energy-per-time unit $P^{ep}_{CGT,t}$ (coming from natural gas), converted in electric active power $P^{el}_{CGT,t}$ and the thermal power $P^{th}_{CGT,t}$

The electrical active power is subject to technical limits

$$0 \le P^{el}_{CGT,t} \le P^{el,\max}_{CGT} \tag{1}$$

Both the thermal power and the primary energy can be linked to the electric power produced by means of a relation that can be assumed to be linear, i.e.

$$P^{\alpha}_{CGT,t} = c^{\alpha}_{CGT} P^{el}_{CGT,t} + b^{\alpha}_{CGT} \tag{2}$$

where α stays for the string "*th*" or "*ep*", while $C^{\alpha}_{CGT}$ and $b^{\alpha}_{CGT}$ are suitable coefficients.

### 3.3 Gas Heater (GH) and Biomass Heater (BH)

The model of these two heater units is substantially the same and very similar to the model introduced for the CGH unit. The model involves again primary energy per time unit $P^{ep}_{\beta,t}$ and the thermal power $P^{th}_{\beta,t}$, with β a string that stays for "GH" and "BH". Here the thermal power is constrained by technical limits to

$$P^{th,\min}_{\beta} \le P^{th}_{\beta,t} \le P^{th,\max}_{\beta} \tag{3}$$

and linked the primary energy per time unit by

$$P^{ep}_{\beta,t} = c^{th}_{\beta} P^{th}_{\beta,t} + b^{th}_{\beta} \tag{4}$$

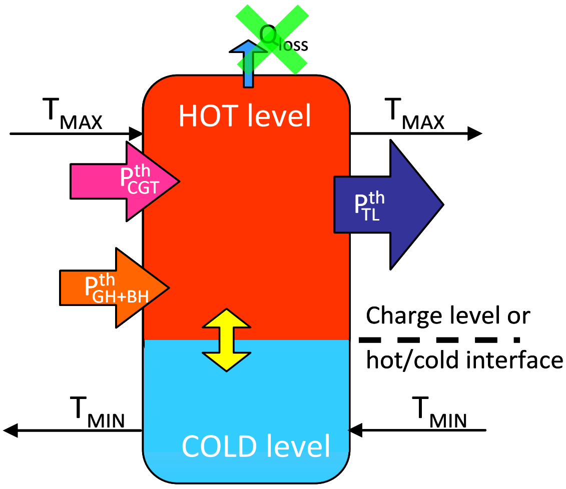


**Figure 2.** Thermal storage model. The open system is described as an energy storage of battery type where only two temperature levels are present

with $C^{th}_{\beta}$ and $b^{th}_{\beta}$ suitable coefficients.

### 3.4 Electrical Storage (ES) and Thermal Storage (TS)

Although these two units operate in different worlds and with different logics, a simple common model able to describe their behavior can be adopted: the ES is represented by the active power $P^{el}_{ES,t}$ and the its energy content $W^{el}_{ES,t}$ related by the continuity equation; the TS which can be seen, from a thermodynamic point of view, as a closed system where only energy flows occur, is described by the exchanged power $P^{th}_{TS,t}$ and its energy content $W^{th}_{TS,t}$ according to the energy conservation equation. A linear approximation of the differential equation that describe the relation between power and energy can be written as

$$P^{\delta}_{\gamma,t} = \begin{cases} \dfrac{1}{\eta^{\delta,c}_{\gamma}} \dfrac{-W^{\delta}_{\gamma,t} + W^{\delta}_{\gamma,t-1}}{\Delta t} & \text{if } W^{\delta}_{\gamma,t-1} \le W^{\delta}_{\gamma,t} \\ \eta^{\delta,d}_{\gamma} \dfrac{-W^{\delta}_{\gamma,t} + W^{\delta}_{\gamma,t-1}}{\Delta t} & \text{if } W^{\delta}_{\gamma,t-1} > W^{\delta}_{\gamma,t} \end{cases} \tag{5}$$

together with the bounds

$$-P^{\delta,d}_{\gamma} \le P^{\delta}_{\gamma,t} \le P^{\delta,c}_{\gamma} \tag{6}$$

$$W_{\gamma}^{\delta,\min} \le W_{\gamma,t}^{\delta} \le W_{\gamma}^{\delta,\max} \tag{7}$$

where δ stays for the string "*el*" or "*th*" and γ stays for the string "*ES*" or "*TS*". In (5) $n_{\gamma}^{\delta,c}$ and $n_{\gamma}^{\delta,d}$ represent the performance coefficients for the charging and discharging phase of the storage system, respectively; in (6) $P_{\gamma}^{\delta,c}$ and $P_{\gamma}^{\delta,d}$ are the maximum power allowed for the charging and the discharging phase, respectively; in (7) $W_{\gamma}^{\delta,min}$ and $W_{\gamma}^{\delta,max}$ are the minimum and maximum energy stored, respectively. The quantity $W_{\gamma,0}^{\delta}$ represents the initial energy content inside the storage system.

The maximum and minimum energy content of for the TS can be related to its volume $V_{TS}$ and the maximum temperature $T_{max}$ or minimum temperature $T_{min}$ of exercise by means of the following

$$W_{TS}^{th,max} = V_{TS} f_V \rho_w c (T_{max} - T_{ref}) \tag{8}$$

$$W_{TS}^{th,min} = V_{TS} \rho_w c (T_{min} - T_{ref}) \tag{9}$$

where $T_{ref}$ is a suitable reference temperature, $f_v$ represents the useful fraction of ST volume, $\rho_w$ is the water density and $c$ is its specific heat. In Fig. 2 a graphical representation of the TS model is presented.

### 3.5 Electric network

The model adopted for describing the SPM electric network is the Single Bus Bar approximation which assumes that all the generations and loads are positioned to the same bus-bar. As a result, the only power balance equation is the one to be encoded, so that the sum of active powers produced has to satisfy the electrical load $P_{EL,t}^{el}$ at each instant time *t*:

$$P_{RES,t}^{el} + P_{ES,t}^{el} + P_{CGT,t}^{el} + P_{NET,t}^{el} = P_{EL,t}^{el} \tag{10}$$

where $P_{NET,t}^{el}$ is the electrical power exchanged with the external network. It will be useful in the following to split $P_{NET,t}^{el}$ in its positive and negative part, i.e.

$$P_{NET,t}^{el,+} - P_{NET,t}^{el,-} = P_{NET,t}^{el} \tag{11}$$

where $P_{NET,t}^{el,+} = \left[ P_{NET,t}^{el} \right]^{+}$ and $P_{NET,t}^{el,-} = \left[ -P_{NET,t}^{el} \right]^{+}$.

### 3.6 Thermal network

In a similar way, once at disposal the thermal load $P_{TL,t}^{th}$, the thermal network model for the SPM is again written by means of a heat transfer rate balance equation for any instant time *t* as

$$P_{TS,t}^{th} + P_{CGT,t}^{th} + P_{GH,t}^{th} + P_{BH,t}^{th} = P_{TL,t}^{th} \tag{12}$$

Due to the fact that the CGTs are able to discard the thermal power produced, relation (11) can be relaxed to

$$P_{TS,t}^{th} + P_{CGT,t}^{th} + P_{GH,t}^{th} + P_{BH,t}^{th} \ge P_{TL,t}^{th} \tag{13}$$

where the inequalities mean that it could be more convenient, from an economical point of view, use CGTs to generate electrical even if the thermal request has already been satisfied.

### 3.7 Operational cost

The overall energy cost of the SPM in the time window $[\mathrm{N}_1, N_2]$ can be expressed now in terms of electrical and thermal power produced, i.e.

$$C_{N_1}^{N_2} = \Delta t \sum_{t=N_1}^{N_2} \Big[ C_{CGT} P_{\mathrm{CG}T,t}^{ep} + C_{GH} P_{\mathrm{GH},t}^{ep} + \\ + C_{BH} P_{\mathrm{BH},t}^{ep} + C_{NET}^{+} P_{NET,t}^{el,+} - C_{NET}^{-} P_{NET,t}^{el,-} \Big] \tag{14}$$

where $C_{CGT}$, $C_{GH}$ and $C_{BH}$ are the costs of the gas/biomasses per primary energy including the maintenance cost while $\mathrm{C}_{NET}^{+}$ and $\mathrm{C}_{NET}^{-}$ represent the cost of the electrical energy purchased by/sold to the external grid.

## 4. DESIGN CRITERIA FOR THE BOILER AND THERMAL STORAGE

In order to establish which is the best size $P_{BH}^{th,max}$ of a BH and the best volume $v_{TS}$ of a TS to be installed in the SPM, a cost function that takes into account the investment cost $C_0$ to purchase the BH and the TS and the cost associated to the operational cost (13) during the system lifetime has to be defined (see [15]).

The investment cost $C_0$ can be estimated according to:

$$C_0 = C_{0,BH} P_{BH}^{th,\max} + C_{0,TS} V_{TS} \tag{15}$$

being $C_{0,BH}$ and $C_{0,TS}$ the initial cost per unitary size of the BH and TS, respectively.

The cost associated to the operational cost (13) for the whole life of the system has be obtained using one year of historical data collecting the electrical and thermal load as well as the RES power production of the SPM measured with a sampling time of 1h, and repeating the same set of data for the whole life, fixed in 20 years. In Fig. 3 the thermal and electrical load power profile of the SPM for the whole month of February 2017 have been proposed as an example as a function of time.

Since the cost (13) depends on the power produced by each programmable unit, the logic that fixes them minimizing day by day (13) has been selected.

Formalizing what described in the previous paragraphs, one gets the following relations for total life cost of the plant that obviously depends on $P_{BH}^{th,max}$ and $v_{TS}$. In (16) $w$ is the Weighted Average Cost of Capital (here assumed 0.035).

$$C_{life} = C_0 + \sum_{j=1}^{20} \left[ \frac{1}{(1+w)^{j+0.5}} \sum_{j=1}^{365} C_{24(j-1)+1}^{24j} \right] \tag{16}$$

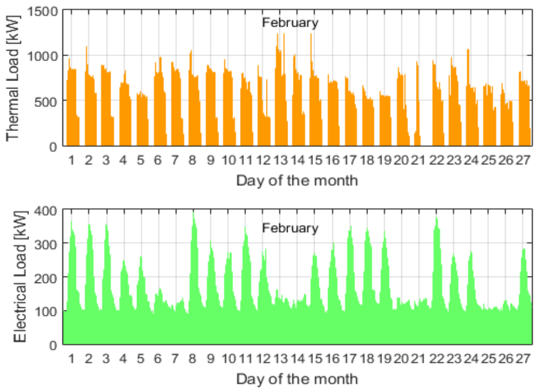


**Figure 3.** Thermal (blue line) and electrical (red line) load profiles for the SPM as a function of time for February 2017

## 5. RESULTS: NUMERICAL EXPERIMENTS WITH HEAT STORAGE SYSTEM AND BIOMASS UNIT

A large number of simulations have been carried out starting from the energy demand historical data for the year 2017. The EMS algorithm was addressed as in its predictive control mode to minimize a cost function on a daily bases and repeating the simulation for a complete year. The main parameter of the simulation was the thermal storage size, being selected the BH nominal capacity at 200kW. The storage size was varied in the range 10 to 100 m$^3$, even if practical considerations about the availability on place of such a space probably will suggest to limit the size to 50 m$^3$ maximum.

Some additional simulations have been run from a pure energy saving point of view. In such a case the aim was to maximize the cogeneration of the gas turbines that currently are producing electricity but not cogenerating at night (from 10pm to 5.30am) since no thermal load is scheduled in this period (building heating system is off at night, see for example Fig. 4).

The campus heating demand in 2017, taking as a reference a typical day in the November to February period, ranged from 5500 kWh to 7900kWh, being the highest demand the one related to the month of January. Fig. 5 shows the results of this analysis.

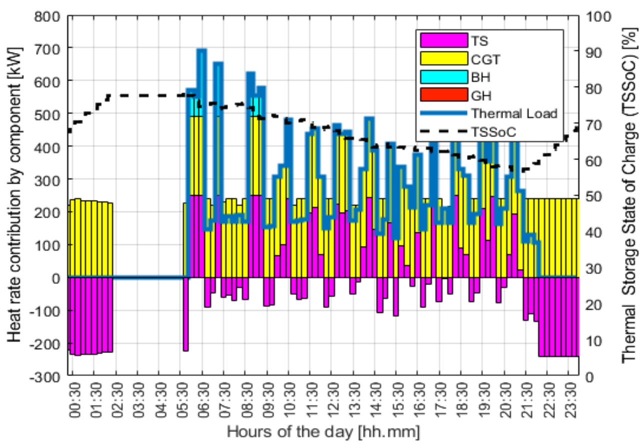


**Figure 4.** Heat transfer rate contributions by component as a function of time for the 26th of February, 2017. Negative values represent the charging periods of the TS. On the secondary axis the TS state of charge is represented. Storage volume 60m$^3$

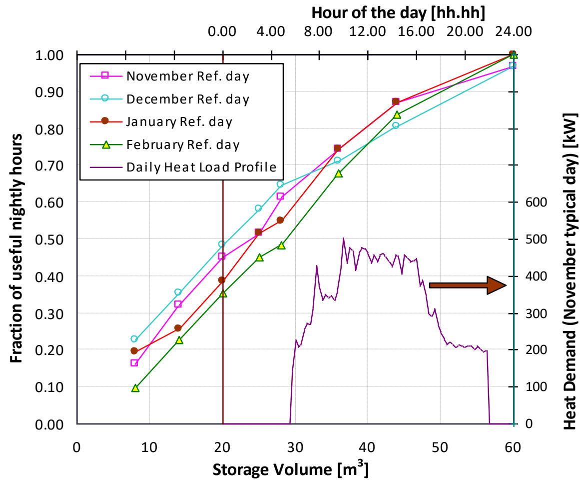


**Figure 5.** Fraction of nightly hours in cogeneration mode by the CGTs as a function of the storage volume. Typical days per month are considered in terms of temporal heat demand profile. Second axes: typical November day heat profile

Here the fraction of the above night hours along which the CGTs are delivering heat to the storage is presented as a function of the storage volume, for 4 typical daily heat loads. The same picture shows the profile of one of those daily heat profile, namely the reference day profile for November (left y axis and top x one). As can be immediately noticed, at a storage volume equal to 60 m$^3$ the gas turbines are allowed to run all night long in cogeneration mode, being the storage able to accept the whole amount of energy available from CGTs. The month by month profile refer to a typical day in terms of heat demand profile that is a sort of average of the complete monthly series (cf. Fig. 3).

Fig. 4 takes into a consideration a low demand day at the end of February and a storage volume of 60 m$^3$. In this figure the heat transfer rate contributions per component are presented as a function of time. It can be observed that the CGT are cogenerating continuously during the day (from 5.30am to 10pm) while only a fraction of the nightly hours are fully employed. In the above figure the TS negative values represent periods when the CGTs is “charging” the TS (say the TS is absorbing energy). The figure also shows the state of charge of the thermal storage (TSSoC) and its daily profile, starting and ending as requested at the same level. In this particular day of February, only some 60% of the nightly hours are employed for cogeneration. In this particular case the overall heat demand (quite flat over time) is almost fully covered by the CGTs and no room for much heat storage is possible.

Fig. 6 shows the profile of the overall cost for the refurbishment of the heating system with BH and TS with the BH and TS capacity as a parameter. The overall cost, including the capital, operational, O&M and financial cost is evaluated according to the algorithm described in Section 4. It is apparent from the figure that the optimum TS size in terms of cost saving is around 60 m$^3$, almost irrespective of the BH capacity. The figure also shows that the overall cost is always decreasing as the storage volume is increased up to the optimum value and that from a 10 m$^3$ volume on the intervention (BH and TS) is beneficial with respect to the base solution which represents the current situation (No BH curve). These findings are in agreement with the energy analyses described previously (i.e. Fig. 5) and show that exploitation of the night cogeneration can cover the cost related to the new installations.

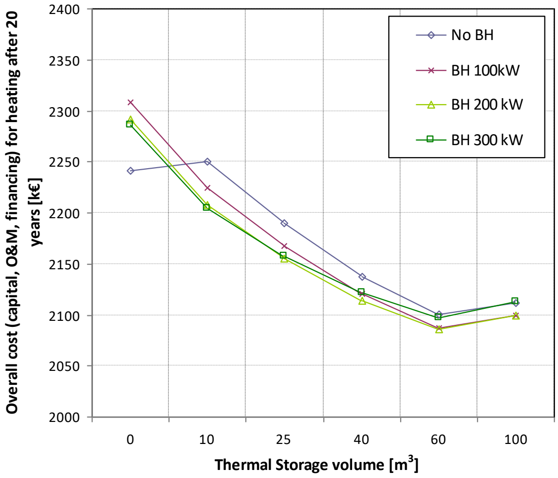


**Figure 6.** Overall cost for heating system (TS and BH) after 20 years of operations

## 6. CONCLUSIONS

The present study has been conceived in order to develop an enhanced version of the Energy Management System which supervises and governs energy flows within the Polygeneration Micro Grid of the University of Genova, Italy. The work has been focused on the prediction of the overall economic performance of the system, considering a possible new configuration, in which a thermal storage and a biomass boiler are included. In this case, the thermal storage goal is to allow night cogeneration by the existing gas turbines, while the biomass boiler should partially replace the existing gas boilers. It is worth noting that the heat storage has been represented by resorting to a new battery-type model able to predict the transient behavior of the grid according to historical series of heat and electricity demand data during the year 2017. In such a way, it has been possible to calculate the optimal size of the thermal storage which maximizes the global saving, demonstrating thus the benefits of the insertion within the Polygeneration Micro Grid of the new thermal storage and biomass boiler components.


## ACKNOWLEDGMENTS

Dr. Beatrice Verduci is greatly acknowledged for the contribution she provided to the present investigation during her MSc Thesis.


## REFERENCES


[1] Dincer I, Rosen M. (2011). Thermal energy storage: Systems and applications. 2nd ed., John Wiley & Sons, Ltd, UK: Chichester.
[2] John A. Duffie WA. (2013). Beckman, Solar Engineering of Thermal Processes. 4th ed., Wiley, Ch. 8.
[3] Haller MY, Cruickshank CA, Streicher W, Harrison SJ, Andersen E, Furbo S. (2009). Methods to determine stratification efficiency of thermal energy storage processes – Review and theoretical comparison. Solar Energy 83: 1847–1860.
[4] Al-Najem NM, El-Refaee MM. (1997). A numerical study for the prediction of turbulent mixing factor in thermal storage tanks. Appl. Therm. Eng. 17(12): 1173-1181.
[5] Panthalookaran V, Heidemann W, Müller-Steinhagen H. (2007). A new method of characterization for stratified thermal energy stores. Solar Energy 81: 1043–1054.
[6] Jannatabadi M, Taherian H. (2012). An experimental study of influence of hot water consumption rate on the thermal stratification inside a horizontal mantle storage tank. Heat Mass Transfer 48: 1103–1112. https://doi.org/10.1007/s00231-011-0958-6
[7] Andersen E, Furbo S, Hampel M, Heidemann W, Muller-Steinhagen H. (2007). Investigations on stratification devices for hot water heat stores. Int. J. Energy Res. 32: 255–263. https://doi.org/10.1002/er.1345
[8] Erdemir D, Altuntop N. (2016). Improved thermal stratification with obstacles placed inside the vertical mantled hot water tanks. Appl. Therm. Eng. 100: 20–29.
[9] Steinert P, Göppert S, Platzer B. (2013). Transient calculation of charge and discharge cycles in thermally stratified energy storages. Solar Energy 97: 505–516.
[10] Baeten B, Confrey T, Pecceu S, Rogiers F, Helsen L. (2016). A validated model for mixing and buoyancy in stratified hot water storage tanks for use in building energy simulations. Appl. En 172: 217–229.
[11] Rosen MA. (2001). The exergy of stratified thermal energy storages. Solar Energy 71(3): 173–185.
[12] Castell A, Medrano M, Solé C, Cabeza LF. (2010). Dimensionless numbers used to characterize stratification in water tanks for discharging at low flow rates. Ren. En. 35: 2192-2199.
[13] Njoku HO, Ekechukwu OV, Onyegegbu SO. (2016). Comparison of energy, exergy and entropy generation-based criteriafor evaluating stratified thermal store performances. Energy and Buildings 124: 141–152.
[14] Bracco S, Brignone M, Delfino F, Procopio R. (2017). An energy management system for the Savona campus smart polygeneration microgrid. IEEE System Journal 11(3): 1799-1809. https://doi.org/10.1109/JSYST.2015.2419273
[15] Bendato I, Bonfiglio A, Brignone M, Delfino F, Pampararo F, Procopio R, Rossi M. (2018). Design criteria for the optimal sizing of integrated photovoltaic-storage systems. Energy 149: 505-515. https://doi.org/10.1016/j.energy.2018.02.056


## NOMENCLATURE

| | |
|---|---|
| RES | Renewable Energy sources |
| CGT | Cogenerative Gas Turbine |
| GH | Gas Heater |
| BH | Biomass Heater |
| ES | Electrical Storage |
| TS | Thermal Storage |
| EL | Electrical Load |
| TL | Thermal load |
| c | specific heat [J/kg/K] |
| t | time [s] |

| | |
|---|---|
| $\Delta$ | Time interval amplitude [s] |

**CGT symbols**

| | |
|---|---|
| $\alpha$ | string "*th*" or "*ep*" |
| $P_{CGT}^{el,max}$ | CGT maximum power [kw] |
| $P_{CGT,t}^{ep}$ | CGT primary energy per time unit at time t [kW] |
| $P_{CGT,t}^{el}$ | CGT electrical power at time t [kW] |
| $P_{CGT,t}^{th}$ | CGT thermal power at time t [kW] |
| $C_{CGT}^{\alpha}$ | CGT constant |
| $b_{CGT}^{\alpha}$ | CGT constant |
| $C_{GHT}$ | GH/BH cost per primary energy [€/kWh] |

**GH/BH symbols**

| | |
|---|---|
| $\beta$ | string "*BH*" or "*GH*" |
| $P_{\beta}^{th,min}$ | GH/BH minimum power [kW] |
| $P_{\beta}^{th,max}$ | GH/BH maximum power [kW] |
| $P_{\beta,t}^{ep}$ | GH/BH primary energy per time unit at time t [kW] |
| $P_{\beta,t}^{th}$ | GH/BH thermal power at time t [kW] |
| $C_{\beta}^{th}$ | GH/BH constant |
| $b_{\beta}^{th}$ | GH/BH constant |
| $C_{\beta}$ | GH/BH cost per primary energy [€/kWh] |
| $C_{0,BH}$ | BH cost per unitary size [€/kW] |

**ES/TS symbols**

| | |
|---|---|
| $\delta$ | string "*th*" or "*el*" |
| $\gamma$ | string "*ES*" or "*TS*" |
| $W_{\gamma}^{\delta,mAX}$ | ES/TS minimum energy [kWh] |
| $W_{\gamma}^{\delta,min}$ | ES/TS maximum energy [kWh] |
| $W_{\gamma,t}^{\delta}$ | ES/TS energy content at time t [kWh] |
| $P_{\gamma,t}^{\delta}$ | ES/TS power at time t [kW] |
| $P_{\gamma}^{\delta,d}$ | ES/TS maximum power discharging [kW] |
| $P_{\gamma}^{\delta,c}$ | ES/TS maximum power charging [kW] |
| $n_{\gamma}^{\delta,c}$ | ES/TS charging efficiency |
| $n_{\gamma}^{\delta,d}$ | ES/TS discharging efficiency |
| $V_{TS}$ | Volume TS [$m^3$] |
| $C_{0,TS}$ | TS cost per unitary volume [€/m3] |
| $\rho$ | density [$kg/m^3$] |

**RES symbols**

| | |
|---|---|
| $P_{RES,t}^{el}$ | RES power at time t |

**NET symbols**

| | |
|---|---|
| $P_{NET,t}^{el}$ | NET power [kW] |
| $P_{NET,t}^{el,+}$ | Power bought from the NET [kw] |
| $P_{NET,t}^{el,-}$ | Power sold to the NET [kW] |
| $C_{NET}^{-}$ | Cost of energy sold [€/kWh] |
| $C_{NET}^{+}$ | Cost of energy purchased [€/kWh] |

**Economic symbols**

| | |
|---|---|
| w | Weighted Average Cost of Capital |